THESIS FOR THE DEGREE OF LICENTIATE OF PHILOSOPHY

Radiation in simulations of high intensity laser-matter interaction

Erik Wallin

Department of Physics
CHALMERS UNIVERSITY OF TECHNOLOGY

Gothenburg, Sweden 2016

Radiation in simulations of high intensity laser-matter interaction
Erik Wallin

Department of Physics
Chalmers University of Technology
SE-412 96 Gothenburg
Sweden
Telephone: +46 (0)31-772 1000

Chalmers Reproservice
Gothenburg, Sweden 2016

Radiation in simulations of high intensity laser-matter interaction
ERIK WALLIN
Department of Physics
Chalmers University of Technology

Abstract

We consider electromagnetic waves propagating in plasmas, with two main themes covered. First nonlinear plasma theory and wave-wave interaction. Here a wave-wave symmetry, the Manley-Rowe relations, is used as a method of determining the physicality of modified plasma fluid equations.

Secondly, we consider radiation emission in simulations of laser-matter interaction where we develop a method of calculating high frequency radiation from relativistic particles, which is not included in particle-in-cell simulations. This is benchmarked against radiation reaction losses and also used in order to compare the radiation between cases where either classical or QED equations of motion are used.

KEYWORDS: plasma, nonlinear dynamics, Manley-Rowe, particle-in-cell, synchrotron radiation, radiation reaction

Publications

This thesis is based on the following publications:

1. **Three-wave interaction and Manley-Rowe relations in quantum hydrodynamics**
   E. Wallin, J. Zamanian, G. Brodin
   J. Plasma Phys. **80** 643 (2014).

2. **Effects of high energy photon emissions in laser generated ultra-relativistic plasmas: Real-time synchrotron simulations**
   E. Wallin, A. Gonoskov, M. Marklund
   Phys. Plasmas **22**, 033117 (2015).

3. **Narrowing of the emission angle in high-intensity Compton scattering**
   C.N. Harvey, A. Gonoskov, M. Marklund, E. Wallin
   Phys. Rev. A **93**, 022112 (2016).

Other publications by the author that are not included in the thesis:

- **Scalar Wigner theory for polarized light in nonlinear Kerr media**
  T. Hansson, E. Wallin, G. Brodin, M. Marklund
  J. Opt. Soc. Am. B **30**, 1765 (2013).

- **Extended particle-in-cell schemes for physics in ultrastrong laser fields: Review and developments**
  A. Gonoskov, S. Bastrakov, E. Efimenko, A. Ilderton, M. Marklund, I. Meyerov, A. Muraviev, A. Sergeev, I. Surmin, E. Wallin
  Phys. Rev. E **92**, 023305 (2015).

Contents

Chapter 1

Introduction

The main theme in this thesis is modelling of radiation in laser-plasma interaction. Mainly the numerical modelling of the emission of synchrotron radiation from relativistic particles in a plasma interacting with a super-intense laser will be covered. However, we will also consider nonlinear wave-wave interaction in a magnetised plasma.

Since the invention of chirped pulse amplification [1] in the 1980s the maximum intensity of lasers has seen a steady increase. Present laser systems are able to focus ultra short pulses with a duration of the order of $\sim 10fs$ to spot sizes of $\sim 1\mu$m (e.g. Hercules [2] with a duration of 30 fs and a spot size of 1.3μm). The total energy of these pulses is not so big, of the order of 1-10 J, but the short duration and small spot size means the maximum intensity is of the order of $10^{22} - 10^{23}$ W/cm^2. This intensity is equivalent to focusing all sun light that reach the earth to a spot size of ≈ 1 mm^2. When such an intense laser pulse hit something, be it a metal or a gas, the atoms will be ionized to form a plasma. For the most intense lasers the prepulse, even if it is much less intense than the main pulse, will be of sufficient intensity to ionize atoms, and the target is already a plasma when the main pulse arrives. Thus the study of ultra-intense lasers interacting with matter is the study of laser-plasma interaction.

Many of the effects in laser-plasma interactions are highly nonlinear and difficult to analyse analytically. For such problems computer simulations are a great tool. These may be of different types, e.g. single-particle codes, Vlasov codes and particle-in-cell (PIC) codes. The PIC method [3, 4] has become a standard method for simulations of laser-plasma interaction. Here the plasma is modelled as an ensemble of particles moving in an electromagnetic field defined on a grid. For each iteration the charge- and current densities are weighted to the grid. These are then used to solve the updated fields and the forces from these fields are weighted back to the particles, which propagate according to their equation of motion, and the process is repeated.

As we will see, particles whose velocity approach the speed of light, c, emit electromagnetic radiation with a typical frequency

$$\omega_c = \frac{3}{2}\omega_H \gamma^3 \tag{1.1}$$

where ω_H is the instantaneous cyclotron frequency of the particle and $\gamma = (1 - v^2/c^2)^{-1/2}$ is the relativistic Lorentz factor. For $\gamma \gg 1$ the radiation is of very high frequency, which the PIC scheme is unable to reproduce. Practically there is the problem that the space and time resolution of the grid provide a limit of how small wavelengths (large frequencies) can be resolved. More importantly, there is a fundamental limitation in the PIC scheme due to the fact that it is the macroscopic properties of the plasma that are simulated. For the scheme to give correct results for high intensity simulations, single particle effects like this must instead be handled in some other way. This will be discussed in this thesis, and Paper II and III provide numerical methods for extending the validity of the particle-in-cell scheme. This is important in order to properly model the physics in extreme laser-matter interaction.

The outline is as follows. Chapter 2 gives an introduction to plasma theory, presenting the properties and main equations governing a plasma as well as examples of linear plasma waves and nonlinear effects. The final section of the chapter gives an introduction to paper I, on three-wave interaction and Manley-Rowe relations in quantum hydrodynamics. Chapter 3 describes the particle-in-cell method of plasma simulations and problems related to including all relevant radiation in simulations of high intensity laser-matter interaction. Chapter 4 covers the theory of electromagnetic radiation with a focus on the radiation from relativistic particles as well as radiation reaction, the back reaction on the radiating particle. In chapter 5 the numerical methods for calculation of high frequency radiation used in papers II and III are presented. Finally, chapter 6 contains a summary of the papers included in the thesis.

The three papers covered in this thesis all adapt a different system of units, SI, Gaussian CGS and natural units; all depending on the convention in their respective subfield. In this thesis I will adapt Gaussian CGS units in general, except in section 2.5 covering details of Paper I where SI units will be used.

Chapter 2

Plasma

A plasma is an ionized gas. Most plasmas are weakly coupled, such that the kinetic energy of a particle is greater than the potential energy due to the nearest neighbour [7]. Heating a gas, eventually the electrons will separate from the atoms to form a gas of electrons and ions, i.e. a plasma. Plasma is often referred to as the forth state of matter and if we look around in the universe we see that it is by far the most abundant, with e.g. our sun constituting a plasma.

2.1 Plasma properties

The fact that the particles in the plasma are electrically charged makes the properties of a plasma vastly different from a gas. The movement of the charged particles will give rise to electromagnetic (EM) fields, and these fields will in turn affect the motion of the particles. One important plasma concept is that of *Debye shielding* [8, 9]. If one introduce a test charge q_T in a plasma of density n and temperature T the surrounding particles will be affected by the field from the test charge and will move to try to cancel this field. This shielding is more efficient the denser and colder the plasma is, and the effect is that the test charge is effectively shielded a few distances λ_D away, where the *Debye length* is given by

$$\lambda_D = \sqrt{\frac{kT}{4\pi n e^2}} \tag{2.1}$$

where k is Boltzmann's constant and $-e$ the charge of the electron. In Fig. (2.1) the electric potential for a free charged particle and the effect of Debye shielding on a charged particle in a plasma can be seen, where there is an additional exponential drop such that for particles a distance $r \gg \lambda_D$ away the test charge is effectively shielded. It turns out that another way to define what is a plasma is to demand that a cube with the sides of the Debye length should contain many particles, $n\lambda_D^3 \gg 1$ (if this was not true then

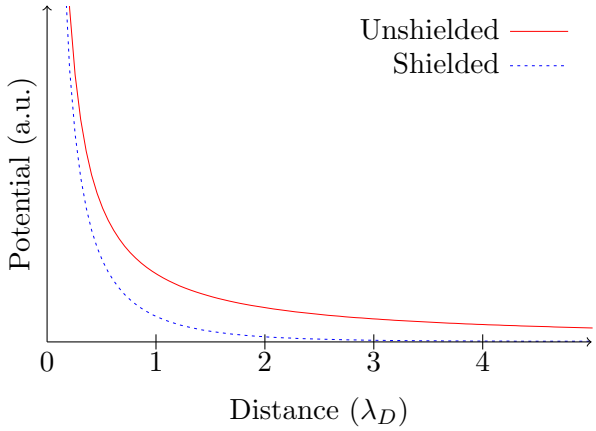

Figure 2.1: The figure shows the electric potential of a point charge with and without Debye shielding.

there would be no particles there to do the shielding). This is equivalent to demanding that the typical kinetic energy of the particles should be larger than the typical potential energy due to the nearest neighbour [7].

The fact that the particles in a plasma can generate, and respond to, EM fields enables it to support many different types of waves, especially if one apply an external magnetic field. If we consider an ion-electron plasma the ions are much heavier than the electrons, with e.g. the proton being ~ 2000 times heavier than the electron. This makes the electrons much more mobile and unless the considered waves are of low frequency, the ions will not have time to move and can be regarded as a neutralizing background with all the density perturbations due to the electrons. If one introduce a density perturbation for the electrons in an otherwise neutral plasma, the charge separation will give rise to an electric field. This will force the electrons back towards their original position, but due to their velocity they will overshoot in the other direction, creating *plasma oscillations*, oscillating with a frequency given by the *plasma frequency*

$$\omega_p = \sqrt{\frac{4\pi n_e e^2}{m_e}} \tag{2.2}$$

where n_e and m_e are the electron density and mass. If the plasma has a nonzero temperature T these oscillations can propagate in the form of *Langmuir waves*. This can be described by the *dispersion relation*, giving the relation between the frequency ω and wave number k of the wave. For a Langmuir wave the dispersion relation is

$$\omega^2 = \omega_p^2 + 3k^2 v_e^2, \tag{2.3}$$

valid for $v_e \ll \omega_p/k$, where $v_e = k_B T/m$ is the thermal velocity of the electrons. From the dispersion relation one can deduce several important properties of the wave, e.g. group velocity (the speed of a wave envelope) and dispersion (the spreading of a wave envelope).

Another type of wave in a plasma is the *electromagnetic plasma wave*. Similarly to in vacuum this is a wave with a transverse E- and B-field, with the difference that the speed of the wave is affected by the plasma. Here the dispersion relation is given by

$$\omega^2 = \omega_p^2 + k^2 c^2 \tag{2.4}$$

where c is the speed of light and ω_p is the plasma frequency defined in Eq. (2.2). The case of an electromagnetic wave in vacuum can be retrieved by letting the plasma density approach zero, such that $\omega_p \to 0$ with the dispersion relation given by $\omega^2 = k^2 c^2$.

For an electromagnetic wave with frequency ω travelling in vacuum and entering a plasma, the possibility of propagating in the plasma depends on the plasma frequency. If $\omega < \omega_p$ then there are no real solutions for k in Eq. (2.4) and the wave can not propagate in the plasma, but will instead be exponentially damped. On the other hand, $\omega > \omega_p$ gives real valued solutions of k and the electromagnetic wave can propagate in the plasma. Thus, depending on the plasma frequency (and hence directly on the density) the plasma can either be transparent or opaque for EM radiation. For a laser with frequency ω the *critical density* is given by

$$n_{\text{crit}} = \frac{m_e \omega^2}{4\pi e^2} \tag{2.5}$$

where for densities $n \leq n_{\text{crit}}$ the plasma is *underdense* and transparent in the absence of collisions, and for densities $n \geq n_{\text{crit}}$ the plasma is *overdense* and opaque.

2.2 Plasma equations

The two main ways of modelling a plasma are the *kinetic* and *fluid* plasma descriptions.

2.2.1 Kinetic description

In kinetic theory the plasma is described by the distribution functions $f_s(\mathbf{r}, \mathbf{v}, t)$ representing the number of particles of species s, (usually $s = e, i$ for electrons and ions) at position $\mathbf{r}$ with velocity $\mathbf{v}$, at time t. The evolution of this system in time is then given by the *Vlasov equation* [10]

$$\frac{\partial f_s(\mathbf{r}, \mathbf{v}, t)}{\partial t} + \mathbf{v} \cdot \frac{\partial f_s(\mathbf{r}, \mathbf{v}, t)}{\partial \mathbf{r}} + \frac{q_s}{m_s}\left(\mathbf{E} + \frac{\mathbf{v}}{c} \times \mathbf{B}\right) \cdot \frac{\partial f_s(\mathbf{r}, \mathbf{v}, t)}{\partial \mathbf{v}} = 0, \tag{2.6}$$

together with Maxwell's equations

$$\nabla \cdot \mathbf{E} = 4\pi\rho \tag{2.7}$$

$$\nabla \cdot \mathbf{B} = 0 \tag{2.8}$$

$$\nabla \times \mathbf{E} = -\frac{1}{c}\frac{\partial \mathbf{B}}{\partial t} \tag{2.9}$$

$$\nabla \times \mathbf{B} = \frac{4\pi}{c}\mathbf{J} + \frac{1}{c}\frac{\partial \mathbf{E}}{\partial t} \tag{2.10}$$

for the fields, where $\mathbf{E}$ is the electric field, $\mathbf{B}$ is the magnetic field, ρ is the charge density and $\mathbf{J}$ is the current density. The latter two are given from the distribution functions by

$$\rho(\mathbf{r}) = \sum_s q_s \int f_s(\mathbf{r}, \mathbf{v}, t)\mathrm{d}^3 v \tag{2.11}$$

and

$$\mathbf{J}(\mathbf{r}) = \sum_s q_s \int \mathbf{v} f_s(\mathbf{r}, \mathbf{v}, t)\mathrm{d}^3 v \tag{2.12}$$

respectively. The Vlasov equation is probably the most important plasma equation and can describe a large variety of plasma phenomenon. It does not take collisions into account, however for a weakly coupled plasma where $n\lambda_D^3 \gg 1$ the collisional effects are small compared to the collective plasma effects [9].

2.2.2 Fluid description

The fluid description is a simplification of the Vlasov equation, where each species of the plasma is considered an interpenetrating fluid. The equations are derived by taking velocity moments of the Vlasov equation. In principle the result is an infinite series of equations of three dimensions, replacing the six-dimensional Vlasov equation. In practice though, the series is truncated using physical arguments to give a limited amount of equations, typically two or three. Integrating the Vlasov equation over all velocities results in the *continuity equation*,

$$\frac{\partial n_s}{\partial t} + \nabla \cdot (n_s \mathbf{v}_s) = 0 \tag{2.13}$$

with $n_s = n_{e,i}(\mathbf{r})$ and $\mathbf{v}_s = \mathbf{v}_{e,i}(\mathbf{r})$ representing the density and velocity of the electrons and ions respectively. The continuity equation describes the fact that the fluid is not created nor destroyed. Multiplying the Vlasov equation by $\mathbf{v}$ and integrating over all velocities results in the *momentum equation*

$$\frac{\partial \mathbf{v}_s}{\partial t} + (\mathbf{v}_s \cdot \nabla)\,\mathbf{v}_s = -\frac{\nabla P}{n_s m_s} + \frac{q_s}{m_s}\big(\mathbf{E} + \frac{\mathbf{v}_s}{c} \times \mathbf{B}\big) \tag{2.14}$$

describing the effect of forces on the fluid. Fluid theory is a rather crude approximation of kinetic theory. As such there are situations where it is easier to work with and where it gives the same result as kinetic theory. However, the dependence of the velocity distribution is lost and effects where this is of importance can not be calculated using fluid theory, e.g. *Landau damping* [11].

2.3 Linear theory and plasma waves

As mentioned, a plasma supports a multitude of waves. In order to find these solutions we *linearize* the plasma equations; considering small perturbations of the involved parameters, with e.g. the density written as the sum of two components

$$n = n_0 + n_1(\mathbf{r}, t) \tag{2.15}$$

where n_0 is the unperturbed, constant background value and $n_1 \ll n_0$ being a time- and space dependent perturbation. Depending on the considered situation, these assumptions will be different and will result in different wave solutions. We can e.g. consider cases where there is no background magnetic field, where the background magnetic field is along some direction or where the magnetic field plays no part at all, resulting in different wave solutions.

In linear theory we consider the perturbations so small so the product of two perturbations, e.g. $n_1 E_1$, is negligible. Thus we only consider results up to first order in the small perturbations. The result is a system of equations for the involved perturbations and background values, where wave solutions can be found by looking for solutions on the form

$$n_1(\mathbf{r}, t) = \tilde{n}_1 \exp(-i\omega t + i\mathbf{k} \cdot \mathbf{r}) \tag{2.16}$$

where $\tilde{n}_1$ is the amplitude, $\mathbf{k}$ the wave vector and ω the frequency. The complex expression is used for convenience, and as the equations are linear the physical solution can be retrieved by taking the real part in the end. The result is a relation between the frequency ω and the wave vector $\mathbf{k}$, i.e. a dispersion relation, mentioned in section 2.1. This procedure, with appropriate linearization, allow us to derive dispersion relations for a large number of plasma waves (e.g. Langmuir waves, ion-acoustic waves and electromagnetic waves), especially if an external magnetic field is present. A simple example is if we neglect ion motion and linearize according to $n_e = n_0 + n_1(\mathbf{r}, t)$, $E = E_1(\mathbf{r}, t)$ and $v_e = v_1(\mathbf{r}, t)$ we can derive the plasma oscillations $\omega = \pm\omega_p$ mentioned above. For further reading on this, see e.g. [9].

2.4 Nonlinear theory and wave-wave interaction

In nonlinear theory we consider larger perturbations, where the product of two perturbations can no longer be neglected, as they were in linear theory. This opens up for several effects not present in linear theory. One such effect is that of wave-wave interaction, where energy is transferred between interacting waves. This is in contrast to linear theory, where the superposition principle applies and energy can not be transferred between waves in a homogeneous medium.

We consider three interacting waves, with e.g. the electric field given by (and similar for the magnetic field, density and velocity)

$$E = E_{(1)}e^{i(k_{(1)}r-\omega_{(1)}t)} + E_{(2)}e^{i(k_{(2)}r-\omega_{(2)}t)} + E_{(3)}e^{i(k_{(3)}r-\omega_{(3)}t)} + \text{c.c.} \quad (2.17)$$

where c.c. denotes the complex conjugate and $E_{(i)}$, $\omega_{(i)}$ and $k_{(i)}$ denotes the amplitude, frequency and wave number of the i:th wave. Here we must add the complex conjugate to make the expression real from the start, as the real and imaginary parts are not independent solutions as in linear theory. We also consider the following relation between the frequencies and wave vectors of the three waves,

$$\begin{aligned} \omega_{(3)} &= \omega_{(1)} + \omega_{(2)} \\ \mathbf{k}_{(3)} &= \mathbf{k}_{(1)} + \mathbf{k}_{(2)}, \end{aligned} \quad (2.18)$$

which will be necessary in order to derive equations for the evolution of the wave amplitudes. Here one could consider the case of having one wave from the start, entering a plasma region. There will be noise in that region, which could be decomposed into different frequencies. Some of these perturbation can match with the incoming wave according to the relations in Eq. (2.18) and those waves can grow, taking energy from the initial wave.

Entering the expression for the fields, densities and velocities on the form of Eq. (2.17) into the plasma fluid equations, there will be a lot of nonlinear terms that are products of parts from the three different waves. For each term in the fluid equations involving a product of two quantities there will be 6^2 such nonlinear terms (from the 3 real and 3 imaginary terms of each quantity). It turns out that not all of these terms are important when it comes to how the amplitude of each wave will evolve, depending on their timescale. Only terms oscillating with similar frequencies will be of importance, as the other will be out of phase and over a longer time their average contribution will be 0. In order to simplify this, and get expressions for how the amplitude of each wave (represented as the amplitude of e.g. the electric field) will develop, one can filter out the frequency of that wave. By e.g. multiplying Eq. (2.17) by $e^{-i(k_{(3)}r-\omega_{(3)}t)}$ and taking the average over many periods one will single out the $E_{(3)}$ part, as all other terms will be rapid oscillations giving 0 in average, where as the $E_{(3)}$ part will be

constant. In a similar manner, using the relations in Eq. (2.18) one can single out contributing nonlinear terms in the fluid equations. E.g. the term matching with $E_{(3)}$ from $\mathbf{v} \times \mathbf{B}$ will be

$$v_{(2)}B_{(1)} \propto e^{i\left((k_{(1)}+k_{(2)})r-(\omega_{(1)}+\omega_{(2)})t\right)} = e^{i(k_{(3)}r-\omega_{(3)}t)}. \tag{2.19}$$

In this manner, we can eventually get equations for how the wave amplitudes will evolve, on the form

$$\frac{\mathrm{d}E^*_{(3)}}{\mathrm{d}t} = c_3 E_{(1)} E_{(2)} \tag{2.20}$$

$$\frac{\mathrm{d}E_{(2)}}{\mathrm{d}t} = c_2 E^*_{(3)} E_{(1)} \tag{2.21}$$

$$\frac{\mathrm{d}E_{(1)}}{\mathrm{d}t} = c_1 E_{(2)} E^*_{(3)} \tag{2.22}$$

where we have used linear relation to express all the nonlinear terms as the same variable (the electric field in this case). c_i represent the coupling coefficients, describing how the different waves couple to each other.

It turns out that there is a restriction in how the waves can exchange energy, i.e. the coupling coefficients c_i must have certain symmetries. These are called the *Manley-Rowe relations* [12] and state that the change in energy of each wave is directly proportional to its frequency. Thus the way the waves can exchange energy is limited, with the effect being that one can consider them exchanging energy similar to quantum theory, one wave quanta at the time.

2.5 Manley-Rowe relations for quantum hydrodynamics

If we denote the total energy of each wave $W_{(i)}$, then the Manley-Rowe relations can be written as

$$\frac{1}{\omega_{(3)}}\frac{\mathrm{d}W_{(3)}}{\mathrm{d}t} = -\frac{1}{\omega_{(1)}}\frac{\mathrm{d}W_{(1)}}{\mathrm{d}t} = -\frac{1}{\omega_{(2)}}\frac{\mathrm{d}W_{(2)}}{\mathrm{d}t}. \tag{2.23}$$

Thus the change in energy of each wave is proportional to its frequency. The Manley-Rowe relation is fulfilled for all the common plasma equations, e.g. the Vlasov equation and the fluid equations described previously. The fact that an equation fulfil the Manley-Rowe relations is related to an underlying Hamiltonian mathematical structure [13, 14].

For a physical theory to be sound, one often demand it to fulfil a number of relations, such as conservation of energy, momentum and angular momentum. In Paper I [15] we consider the Manley-Rowe relations as an additional criteria in separating physical from unphysical models, in order

to verify the form of the *Bohm de Broglie* term in quantum hydrodynamics. The momentum equation (here in SI units),

$$\left(\frac{\partial}{\partial t}+\mathbf{v}\cdot\nabla\right)\mathbf{v}=\frac{q}{m}\left(\mathbf{E}+\mathbf{v}\times\mathbf{B}\right)-\frac{\nabla P}{nm}+\frac{\hbar^2}{2m^2}\nabla\left(\frac{1}{\sqrt{n}}\nabla^2\sqrt{n}\right) \quad (2.24)$$

with the Bohm de Broglie term (right most term) represents the simplest quantum hydrodynamic equation [16, 17, 18]. The Bohm de Broglie term is usually small and can be neglected, but for high density, low temperature plasmas [17] it is of importance. Eq. (2.24) can be derived in several ways [18, 19], but none with total mathematical rigour.

We find the Manley-Rowe relations for quantum hydrodynamics, but starting from a more general form of the Bohm de Broglie term

$$\frac{\hbar^2}{2m^2}\nabla\left(\frac{1}{n^\xi}\nabla^2 n^\xi\right) \quad (2.25)$$

with the hope of showing that this is only valid for the case $\xi = 1/2$. From an expression for the total energy of the wave (given by electric, magnetic, kinetic, pressure and Bohm de Brogile contributions) as

$$\begin{aligned} W_{(i)} &= \frac{\epsilon_0}{2}\mathbf{E}_{(i)}\cdot\mathbf{E}^*_{(i)}+\frac{1}{2\mu_0}\mathbf{B}_{(i)}\cdot\mathbf{B}^*_{(i)} \\ &+\sum_s\left[\frac{m_s n_{0s}}{2}\mathbf{v}_{(i)s}\cdot\mathbf{v}^*_{(i)s}+\left(\frac{\gamma_s P_{0s}}{2n_{0s}^2}+\frac{\xi\hbar^2 k_{(i)}^2}{4m_s n_{0s}}\right)n_{(i)s}n^*_{(i)s}\right] \end{aligned} \quad (2.26)$$

we derive expressions for the change in energy of each wave. After some lengthy algebra we arrive at the main result, here expressed for wave 3,

$$\begin{aligned} \frac{\mathrm{d}W_{(3)}}{\mathrm{d}t} &= \omega_{(3)}\sum_s\Bigg[-\frac{im_s}{2}\Big(n_{(1)s}\mathbf{v}_{(2)s}\cdot\mathbf{v}^*_{(3)s}+n_{(2)s}\mathbf{v}_{(1)s}\cdot\mathbf{v}^*_{(3)s} \\ &+n^*_{(3)s}\mathbf{v}_{(1)s}\cdot\mathbf{v}_{(2)s}\Big)-\frac{i\gamma_s(\gamma_s-2)P_{0s}}{n_{0s}^3}n_{(1)s}n_{(2)s}n^*_{(3)s} \\ &+\frac{i\xi\hbar^2}{8m_s n_{0s}^2}\left[k_{(1)}^2+k_{(2)}^2+k_{(3)}^2-(2\xi-1)\mathbf{k}_{(1)}\cdot\mathbf{k}_{(2)}\right]n_{(1)s}n_{(2)s}n^*_{(3)s} \\ &-\frac{m_s\omega_{cs}}{2\omega_{(3)}}n_{0s}\left(\frac{k_{(2)z}}{\omega_{(2)}}-\frac{k_{(1)z}}{\omega_{(1)}}\right)\mathbf{v}^*_{(3)s}\cdot\left(\mathbf{v}_{(1)s}\times\mathbf{v}_{(2)s}\right)\Bigg]+\text{c.c.} \end{aligned} \quad (2.27)$$

Even if it is not entirely trivial to see, all terms except the one proportional to $(2\xi-1)$ are symmetric with respect to the different waves, thus fulfilling the Manley-Rowe relations. For the Manley-Rowe relations to hold in general, that term must be 0, and thus $\xi = 1/2$ as is the case in the Bohm de Broglie term. This adds further weight to the derivation and physical soundness of the equations for quantum hydrodynamics. The the fact that the Manley-Rowe relations is only fulfilled for the case of $\xi = 1/2$ also demonstrates that the Manley-Rowe relations is a useful criterion for separating physical equations from unphysical ones.

Chapter 3

Particle-in-cell scheme

3.1 Classical particle-in-cell scheme

The PIC scheme is a method of plasma simulations [3, 4] which has become a standard tool for large scale plasma simulations. Here the plasma consists of an ensemble of particles moving within a grid representing the simulated space. To advance the system in time, Maxwell's equations (Eqs. 2.7 - 2.10) for the electric- and magnetic field in each grid point and the equation of motion for the particles are solved self consistently.

There are different numerical methods for the field solver (e.g. FDTD [20, 4] or spectral [21] methods) and the position of each component of the field can vary within the grid cell, but for all cases the fields are considered to be placed discretely on the grid, with particles moving continuously (up to computer number precision) there in. The steps in the method can be seen in Fig. (3.1). For each particle and iteration the position and velocity of the particles are weighted to the grid to get the charge- and current densities $\rho(\mathbf{r})$ and $\mathbf{J}(\mathbf{r})$. These are then used in Maxwell's equations in order to update the values of the E- and B-fields. Finally the field values are weighted to the position of each particle and the equation of motion is solved in order to update the position and momentum of the particle, after which the process restarts for another iteration. In a typical simulation the number of particles under consideration is much too great to include all in the simulation, due to memory limitations (e.g. the 10^{18} particles in 1 cm^3 of a typical gas would require $\sim 5 \times 10^7$ TB of memory to store the position and momentum of each particle). In PIC one instead consider *super particles*, each representing a larger number of real particles. However, given a certain field the super particles follow the same path as real particles would do, as the charge to mass ratio is the same. The equation of motion for the particles is given by the Lorentz force, $F = q(\mathbf{E} + \mathbf{v}/c \times \mathbf{B})$, where the *Boris scheme* [22] is the most common *particle pusher*. This is an efficient leap-frog method where first half the acceleration due to the electric field is applied, then a rotation

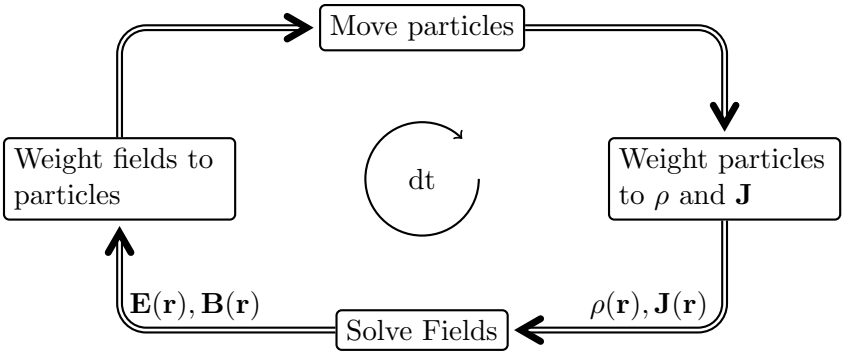

Figure 3.1: The figure shows the classical PIC scheme.

due to the magnetic field and finally the other half of the contribution due to the electric field.

The PIC method has turned out to be applicable for plasma simulations in a large number of regimes, with the original method extended to include e.g. collisions [23] and ionization [24]. However, present and coming [25, 26, 27] high intensity laser facilities present regimes where the PIC method fails to take into account the emission of high frequency radiation. For even further increase in intensity other problems will arise, related to the fundamental change of physics as *quantum electrodynamics* (QED) have to be considered. In the following chapters we will consider the first of these problems.

Chapter 4

Electromagnetic radiation

In classical theory electromagnetic radiation comes in the form of waves, generated from accelerated charges. This is in contrast to quantum theory, where the radiation is considered a particle, the *photon*, with the energy of each photon proportional to its frequency according to $E = hf$ where h is Planck's constant and f the frequency.

We will start in section 4.1 by considering the classical electromagnetic theory and how radiation is emitted from accelerated charges, with a focus on how this can be used in numerical schemes. We will then proceed by looking at the energy loss for an emitting particle, and finally briefly consider the quantum mechanical effect of discrete photon emission. In chapter 5 we consider the implementation of the numerical scheme for emission of classical synchrotron radiation in Paper II [28]. In section 5.2 this is benchmarked to the energy loss due to RR [28] and in section 5.3 a comparison between classical and quantum emission is made, as in paper III [29].

4.1 Radiation from moving charges

The evolution of electric and magnetic fields and their origin are described by Maxwell's equations, Eqs. (2.7-2.10). There is a solution of Maxwell's equations in vacuum where oscillating transverse electric and magnetic fields propagate as a wave with velocity c, the speed of light. The wavelengths of this radiation can vary greatly, with e.g. radio waves in the *kilometer* (10^3 m) wavelength scale and gamma rays in the *picometer* (10^{-12} m) wavelength scale. These waves are generated by the acceleration of charged particles.

Given the path of a charged particle the radiation it emits can be calculated. The energy emitted per unit solid angle and unit frequency interval is given by [5]

$$\frac{\mathrm{d}^2 I}{\mathrm{d}\omega \mathrm{d}\Omega} = \frac{e^2}{4\pi^2 c}\left| \int_{-\infty}^{\infty} \frac{\mathbf{n} \times [(\mathbf{n} - \boldsymbol{\beta}) \times \dot{\boldsymbol{\beta}}]}{(1 - \boldsymbol{\beta} \cdot \mathbf{n})^2} \exp(i\omega(t - \mathbf{n} \cdot \mathbf{r}(t)/c))\mathrm{d}t \right|^2 \quad (4.1)$$

where $\mathbf{n}$ is a unit vector in the direction toward the observer, $\boldsymbol{\beta} = \mathbf{v}/c$ is the particle velocity and $\mathbf{r}(t)$ is the position of the particle. This equation is in the form of an integral over all time (of nonzero acceleration $\dot{\boldsymbol{\beta}}$) and is not suitable to use in numerics, for several reasons. First of all it is very computationally expensive to save particle positions for all time-steps, and secondly this also prevents real time calculation of the emitted radiation.

It turns out that this can be simplified for the case of *relativistic particles*, whose velocity is close to c.

4.2 Radiation from relativistic particles

When the particle velocities v approach the speed of light c, Newtonian theory is no longer valid and one must take effects of special relativity into account. This states that no massive particle can surpass the speed of light, $c \approx 3 \times 10^8$m/s. Many effects in special relativity are proportional to the *Lorentz factor*,

$$\gamma = \frac{1}{\sqrt{1 - \frac{v^2}{c^2}}}, \tag{4.2}$$

where v is the speed of the particle and c is the speed of light. For non-relativistic particles this is very close to unity, but for particles approaching c it grows very quickly, as seen in Fig. (4.1). A particle with velocity very close to c can still be further accelerated to increase its kinetic energy, $E_k = mc^2(\gamma - 1)$ but the predominant effect will not be an increase in its velocity, which will only increase marginally closer to c. Instead effects such as time dilation and length contraction will see the particle measure time and distance differently.

It turns out that for relativistic particles the calculation of emission of radiation can be simplified. The emission from relativistic particles is concentrated withing an angle $1/\gamma$ about its propagation direction. For relativistic particles with $\gamma \gg 1$ we can then to a good approximation consider all radiation as emitted along the propagation direction, removing the angular dependence from the equations. Furthermore, radiation emitted due to *transverse* acceleration ($v \perp a$) is a factor γ^2 greater than that due to *linear* acceleration ($v \parallel a$). This means that for relativistic particles the radiation due to linear acceleration can be neglected [5, 6] and one can consider all the radiation of the particle to be due to transverse acceleration. This opens up the possibility of describing the radiation from a relativistic particle by considering it to be in an instantaneous circular motion, with radius r and circular frequency ω_H.

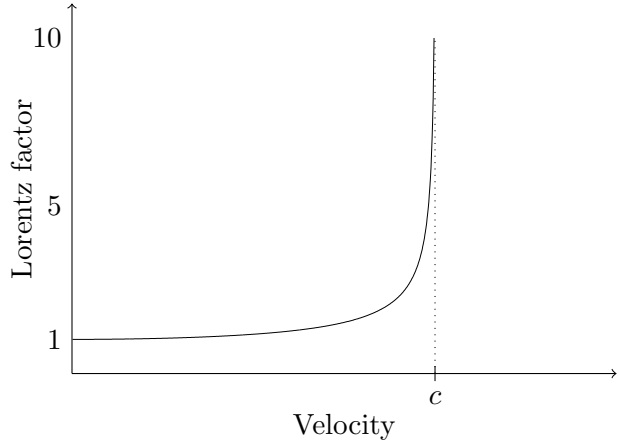

Figure 4.1: The figure shows the relativistic Lorentz factor.

4.2.1 Synchrotron radiation

Synchrotron radiation is the name for radiation emitted from a relativistic particle in circular motion, where $v \perp a$. This can for example be achieved with a charged particle gyrating in an external magnetic field, as seen in Fig. (4.2). We consider an electron going around in a circle of radius r with velocity v. The angular frequency is then given by $\omega_H = v/r$. For a non-relativistic electron the typical frequency of the emitted radiation is $\sim \omega_H$. However, as the the particle becomes relativistic the typical frequency of the emitted radiation is instead ω_c, defined as [6]

$$\omega_c = \frac{3}{2}\omega_H \gamma^3, \tag{4.3}$$

and thus the emitted frequency is greatly increased for particles with $\gamma \gg 1$. The rotation of the particle can be thought of as being due to a perpendicular external magnetic field H_{eff} of field strength

$$H_{\text{eff}} = \frac{\gamma m c \omega_H}{e}. \tag{4.4}$$

The frequency spectra of the emitted radiation can then be written as

$$\frac{\partial I}{\partial \omega} = \frac{\sqrt{3}}{2\pi}\frac{e^3 H_{\text{eff}}}{mc^2} F\left(\frac{\omega}{\omega_c}\right) \tag{4.5}$$

where $F(\xi)$ is the *first synchrotron function* [5, 6] given by

$$F(\xi) = \xi \int_{\xi}^{\infty} K_{5/3}(\xi) \mathrm{d}\xi \tag{4.6}$$

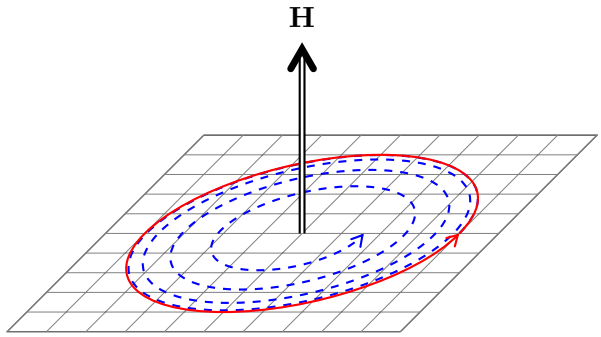

Figure 4.2: The figure shows two cases of a charged particle gyrating in a magnetic field. Blue/dashed line represent the case where radiation reaction is taken into account and the particle loose a substantial amount of energy in each lap due to radiation. Red line represent the case where radiation reaction is not taken into account.

with $K_{5/3}(\xi)$ being a modified Bessel function. This is such that most of the radiation is emitted around the typical frequency ω_c, as seen in Fig. (4.3). Integrating this over all frequencies we get the total radiated power as

$$I = \frac{4e^3 H_{\text{eff}} \omega_c}{9mc^2} = \frac{2e^4 H_{\text{eff}}^2}{3m^2c^3}\gamma^2. \tag{4.7}$$

For a fixed field H_{eff} the power scales as γ^2, thus being dominated by high energy particles.

4.3 Radiation reaction

As a particle emits EM radiation is looses energy. In the non-relativistic case this energy is extremely small compared to the kinetic energy of the particle and can be neglected. For relativistic particles this no longer is the case, and for highly relativistic particles the emitted energy can be a substantial part of the particle kinetic energy and the energy loss must be taken into account in the motion of the particle, see Fig. 4.2. This is the *radiation reaction* (RR) and it has long been a problem how this should be accounted for. In fact, this is where classical electrodynamics fails and for a proper handling one must turn to QED. Even so, there still exist a regime where the effects of radiation reaction can be considered classically. The energy loss due to RR is then relatively small compared to the kinetic energy of the particles and the RR loss can be considered as a continuous friction term (compared to QED where there is a probability of emission, and the process is stochastic). One can add a term for the energy loss due to RR to the

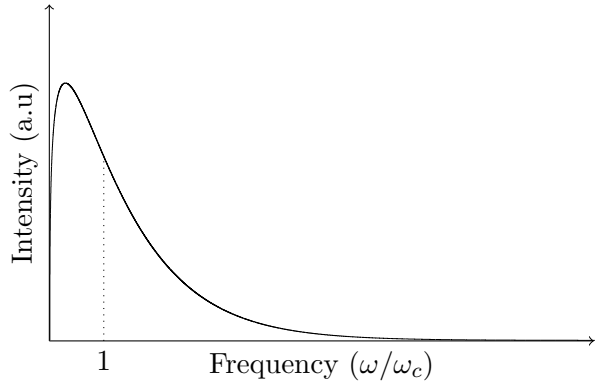

Figure 4.3: The figure shows the spectra of synchrotron radiation

equation of motion of the particle

$$F = F_{\mathrm{EM}} + F_{\mathrm{RR}}. \tag{4.8}$$

where F_{EM} is the Lorentz force. The expression for F_{RR} is then given from demanding that the work performed is the same as the energy of the emitted radiation. This gives the Abraham-Lorentz equation [5] which has the problem of containing a third order derivative. This is untypical in physics and means that is it not enough to specify the initial position and velocity of the particle for the problem to be properly defined, as is customary. Furthermore it allows "runaway solutions", where the particle would be continuously accelerated even without an external force! This is clearly unphysical, but the problem can be removed by approximating the third order derivative using the Lorentz force, F_{EM}. The result is the *Landau-Lifshitz* (LL) equation, valid for $|F_{\mathrm{RR}}| \ll |F_{\mathrm{EM}}|$ in the instantaneous rest frame of the particle. In relativistic covariant form this is given by [6]

$$\begin{aligned} f^{\mu} = & \frac{2}{3}\frac{er_0}{c}\partial_{\gamma}F^{\mu\nu}u_{\nu}u^{\gamma} \\ & + \frac{2}{3}r_0^2\left[F^{\mu\alpha}F_{\alpha\nu}u^{\nu} + (F_{\nu\alpha}u^{\alpha})(F^{\nu\beta}u_{\beta})u^{\mu}\right] \end{aligned} \tag{4.9}$$

where $F^{\mu\nu}$ is the electromagnetic field tensor and $r_0 = e^2/m_e c^2$ is the "classical electron radius". In vector form this becomes

$$\begin{aligned}\mathbf{F}_{\text{rad}} = &\frac{2}{3}\frac{r_0 e}{c}\gamma\left[\left(\frac{\partial}{\partial t} + \mathbf{v}\cdot\boldsymbol{\nabla}\right)\mathbf{E} + \frac{1}{c}\mathbf{v}\times\left(\frac{\partial}{\partial t} + \mathbf{v}\cdot\boldsymbol{\nabla}\right)\mathbf{H}\right] \\ &+ \frac{2}{3}r_0^2\left(\mathbf{E}\times\mathbf{B} + \frac{1}{c}\left[\mathbf{B}\times(\mathbf{B}\times\mathbf{v}) + (\mathbf{v}\cdot\mathbf{E})\mathbf{E}\right]\right. \\ &\left. - \frac{\gamma^2}{c}\left[\left(\mathbf{E} + \frac{1}{c}\mathbf{v}\times\mathbf{B}\right)^2 - \left(\frac{\mathbf{E}\cdot\mathbf{v}}{c}\right)^2\right]\mathbf{v}\right) \end{aligned} \tag{4.10}$$

The LL equation has been shown to be consistent with QED up to first order in the fine structure constant $\alpha \approx 1/137$ [30].

4.4 QED effects

If the energy of the gyrating particle we considered in section 4.2.1 is further increased, then eventually the typical energy $\hbar\omega_c$ of the emitted photons will be comparable to the kinetic energy of the particle. This can be described by the dimensionless parameter

$$\chi = \frac{2\hbar\omega_c}{3\gamma m c^2}, \tag{4.11}$$

where for χ approaching 1 the classical theory is not valid and one must turn to QED. The problem with the classical expressions are two. Firstly, the classical equations of photon emission does not provide a proper cutoff and will eventually predict the emission of photons with greater energy than the kinetic energy of the particle itself, as described by the χ parameter. Secondly, in this regime the energy loss can not be considered a continuous process but must be treated as a stochastic process with a certain probability of emission. Thus a particle, even if it is accelerated, could propagate without emitting radiation for some distance and then emit a substantial part of its energy at some instance. This is in contrast to the classical case where the radiation is emitted continuously, and results in a different dynamics for the particles. According to QED one could imagine a particle moving further into a region of intense electric and magnetic fields (i.e. the focus of a laser pulse) than it would according to the classical theory, as it in each instant is not certain to loose energy due to radiation.

In paper III [29] we consider a relativistic electron colliding with an intense laser pulse and examine the difference in the radiation patterns depending on if the classical- or the QED equations for the particle motion and energy loss are used.

Chapter 5

Numerical methods and results

In the following chapter the numerical methods used in the papers included in the thesis are discussed. The numerical scheme for calculating the emission of high frequency radiation is developed and benchmarked in paper II [28]. This is then applied in comparison with QED in paper III [29].

5.1 Simulations of high intensity laser-matter interaction

In simulations of high intensity laser-matter interaction lasers of intensity up to $10^{23}\mathrm{W/cm}^2$ are considered. These pulses are capable of accelerating electrons to relativistic velocities within a wavelength. As seen in Eq. (4.3) the frequency of the emitted radiation is greatly increased for relativistic particles with $\gamma \gg 1$, and correspondingly the wavelength is decreased.

This poses a problem to the PIC scheme. Not only is there an issue that the spatial and temporal resolutions $\mathrm{d}x$ and $\mathrm{d}t$ provide a cutoff for the radiation that can be resolved by the grid, such that radiation with wavelength $\lambda \leq \mathrm{d}x$ (or frequency $f \geq 1/\mathrm{d}t$) can not be resolved. There is also the fundamental problem that the PIC scheme would not reproduce the correct radiation, even if the grid resolution was greatly improved. This is related to the fact that the PIC idea is to use super-particles, representing a large number of real particles. As they have the same charge-to-mass ratio as real particles they follow the same path as the effect of the Lorentz force is the same. However, not all equations have this simple dependence on charge over mass, with e.g. the intensity of the high frequency radiation in Eq. (4.7) scaling as e^4/m^2. The emission of high frequency radiation can be seen as a single particle, microscopic effect that is not taken into account by the PIC scheme, which instead focus on the collective, macroscopic behaviour of the plasma. In order to include this physics the PIC scheme must be extended.

We solve this by imposing methods of incorporating the radiation in the form of particles.

Classically EM radiation was considered to be a wave, exhibiting wave like properties such as interference in two-slit experiments. Here light going through two nearby slits not only add up, but interfere such as there are spots on the screen behind where the intensity of light is smaller when both slits are open than when one of them is closed. Electrons and protons on the other hand has been considered particles, exhibiting particle like properties such that they come in discrete packages. However, it turned out that there were situations in which the wave description for EM radiation was insufficient and this instead had to be considered as particles, e.g. to explain the cut-off frequency in the *photoelectric effect*. Here light is shone at a metal which then emits electrons as it absorbs the energy of the light. However, below the cut-off frequency no electrons are emitted, independent of the intensity of the light, indicating that the energy is passed in discrete packages, quantas with energy proportional to their frequency. Likewise classical particles such as electrons and protons turned out have wave like properties in certain situations, such as interference in two slit-experiments as mentioned above. This insufficiency of being able to describe these phenomena as either of these two, to us well defined and separate, cases is resolved by QED. Here everything is considered as particles, but whose motion is governed by probabilities given by the square of a corresponding complex amplitude. This regains the discrete nature of particles at the same time as it enable the wave like properties through interference between amplitudes of different outcomes.

Thus, the notion of EM radiation as photons is a quantum description. Here we consider the high frequency radiation to be particles, and we call them "photons" in a more semi-classical fashion, using the simple relation between the frequency f of the light and the energy of the "photon" $E = hf$.

5.2 Monte Carlo method for synchrotron radiation

In order to calculate the emitted radiation from high energy particles we use a *Monte Carlo* (MC) model: We calculate the spectra according to the frequency spectra for synchrotron radiation, Eq. (4.5), and then we *sample* from this through a method involving (pseudo) random numbers. Each emission then involves picking a frequency from the spectra, and emission is determined according to how probable emission of that frequency is. This is a lightweight method where we in average get the correct number of emissions for each frequency interval and can build statistics from this (e.g. frequency and angular spectra).

From values of particle position and momentum before and after the

equation of motion is applied, we can calculate what *efficient magnetic field* H_{eff} this represent. This is the magnetic field, perpendicular to the particle motion, that would cause the same transverse change in the particle momentum, and for a relativistic particle this is given by

$$H_{\text{eff}} = \frac{mc\gamma}{e}\frac{1}{\Delta t}\frac{\sqrt{\mathbf{p}^2 \mathrm{d}\mathbf{p}^2 - (\mathbf{p}\cdot\mathrm{d}\mathbf{p})^2}}{\mathbf{p}^2} \tag{5.1}$$

where $\mathbf{p}$ is the momentum and $\mathrm{d}\mathbf{p}$ the change in momentum of the particle, valid when the change in momentum is much smaller than the momentum, $\Delta p_\perp / p \ll 1$. H_{eff} determines the typical frequency ω_c of the emitted radiation given by

$$\omega_c = \frac{3eH_{\text{eff}}}{2mc}\gamma^2 \tag{5.2}$$

and thus the spectra of the emitted radiation. We wish to pick a frequency ω and using the spectrum $\partial I(\omega)/\partial\omega$ determine if a photon with such a frequency is to be emitted. We want to do this in a clever way in order to reduce noise and speed up computations. On the one hand we wish to allow for picking a wide range of frequencies, but on the other hand we do not want to pick frequencies with extremely small probability of emission too often, as this would be a waste of computational time.

To solve this we generate ω according to a distribution function $S(\omega)$, so that frequencies for which the probability of emission are large are more often selected. This is then compensated for by decreasing the probability of emission by the corresponding values. In order to do this numerically, without resorting to tabulated values, one need a function which is easily integrable, which is not the case for the synchrotron function. However, we can construct a simplified function $S(x)$ using the asymptotic values of the synchrotron function. Thus our simplified function approaches the values of the synchrotron function for the extreme cases of $\omega \to 0$ and $\omega \to \infty$. This function is chosen as

$$S(x) = \begin{cases} 4/3x^{1/3} & \text{if } x < a, \\ 7/9e^{-x} & \text{if } x > a, \end{cases} \tag{5.3}$$

where the constant $a \approx 0.69021$ is determined such that $\int_0^\infty S(x) = 1$. We can then calculate

$$P(\omega) = \int_0^\infty S(x)\mathrm{d}x \tag{5.4}$$

and find its inverse $\omega(P)$ such that we can pick the frequency as $\omega = \omega(R)$ where R is a (pseudo) random number $R \in [0, 1]$. The number of photons of frequency ω is then given by

$$\mathrm{d}N = \frac{\frac{\mathrm{d}I}{\mathrm{d}\omega}(\omega)}{\hbar\omega S(\omega/\omega_c)}\Delta t \tag{5.5}$$

where Δt is the time-step. If a photon should be emitted is then determined by comparing $\mathrm{d}N$ to another (pseudo) random number $R' \in [0, 1]$, where a photon is emitted if $\mathrm{d}N \geq R'$.

The scheme is limited in that it does not take interference between emission at different time-steps into account. However, for applications in high intensity laser matter interaction it is reasonable to neglect this [28].

Also, even if the approximation used in Eq. (5.1) is generally very good for relativistic particles, situations can occur in PIC simulations where it is violated, due to the Boris scheme particle pusher. One can imagine rare events where a particle is decelerated to a low energy by the first half of the electric field, and because of this it is then greatly rotated by the magnetic field. When the final half of the electric field then is applied the particle momentum will have turned completely. This gives a large change in momentum $\Delta p_\perp$ and a small average momentum p, greatly overestimating H_{eff} with the effect of rare, much too energetic emissions. We solve this issue by imposing the limit $\Delta p_\perp / p \leq 1$ in the calculation of H_{eff}.

5.2.1 Benchmarking for Laser Wakefield Acceleration

We use the method of radiation emission in two papers. In paper II [28] the method is developed and implemented into the PIC-code *ELMIS* [32] and we perform benchmarking against the radiation loss calculated by the Landau-Lifshitz equation, Eq. (4.10), for the case of the bubble regime [33] of laser wakefield acceleration (LWFA) [34, 35]. This is a highly nonlinear process where an intense laser is shot at a underdense plasma. As the pulse enters the plasma the *ponderomotive force* acts to force the light electrons away from the pulse region, with the heavier ions remaining as a charged background. This sets up a strong electric field [36, 37, 38], quickly accelerating electrons behind the pulse to velocities close to the speed of light. The electrons follow the laser pulse, accelerating to higher and higher energies [39, 40], as well as radiating high frequency radiation [41, 42]. An illustration of this can be seen in Fig. (5.1). In Fig. (5.2) the comparison between the energy loss of the particles as given by the RR force and the emitted energy as calculated by Eq. (5.5) can be seen, with excellent agreement between them.

5.3 Classical v. quantum radiation emission.

In paper III ([29]) we also make use of the developed scheme for calculation of synchrotron radiation. Here the scheme is implemented in the single particle code *Simla* [43]. In contrast to the PIC method, here we consider only one particle interacting with an intense laser pulse. The contribution of this single particle to the fields is negligible and instead of self consistently solving Maxwell's equations on a grid as done in the PIC scheme, here we use analytical expressions for the laser pulse. This gives the possibility of

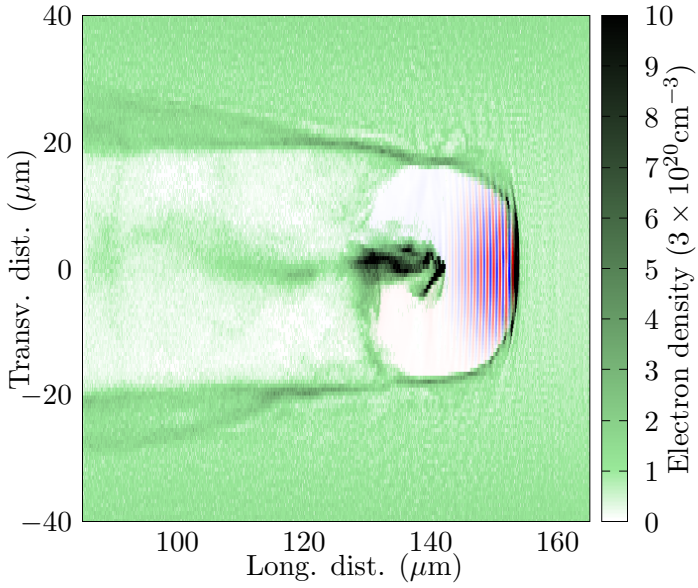

Figure 5.1: The figure shows the electron density (green-black) and laser pulse (red-blue) for a 3D PIC LWFA simulation.

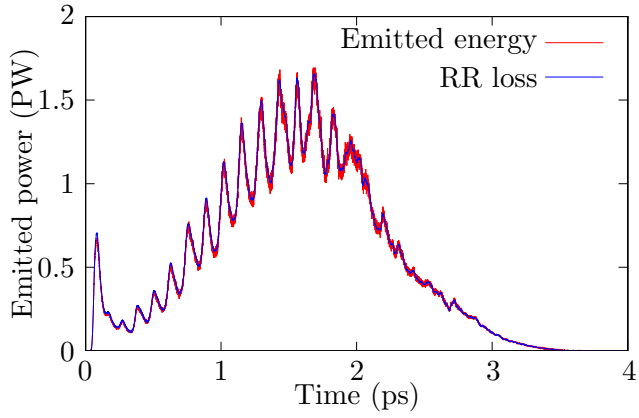

Figure 5.2: The figure shows a comparison between the energy loss due to RR (blue) and the energy of the radiation emitted by the Monte Carlo synchrotron radiation scheme (red).

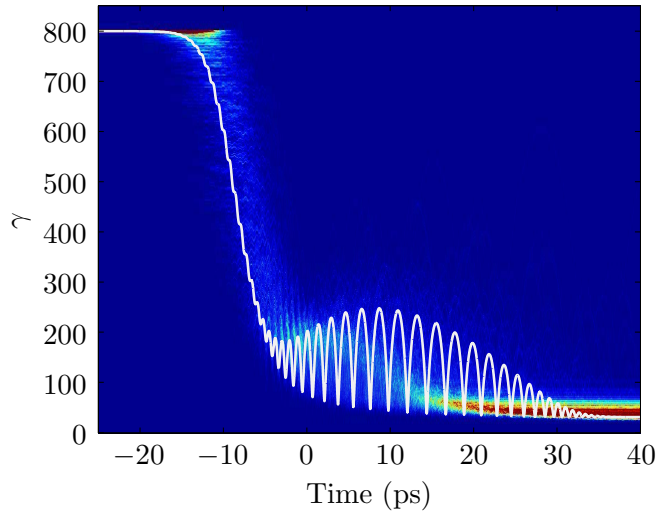

Figure 5.3: The figure shows the gamma value of the electron as a function of time, as it collides with the laser pulse. The white line is for a classical equation of motion and the heat map (blue to red) is from a number of QED runs.

modelling realistic laser pulses with very small time-steps for the particle motion.

Simla allows for simulation using either a classical or a QED corrected equation of motion for the particle. The quantum version uses equations for emission from QED together with (pseudo)random numbers to model emission. The effect is that the particles does not loose energy continuously as in the classical case, but rather in discrete emissions. The particle can then propagate a certain distance without radiating, and then emit a large part of its energy as radiation during one time-step. This process is not deterministic, and we run a large number of QED runs to get a representative picture of the process.

We consider the head-on collision between a laser pulse and an electron. As a first step the laser pulse is given by a idealistic Gaussian shape with relativistic amplitude $a_0 = 200$, with the electrons having $\gamma = 800$. As the electron meets the pulse its energy is decreased, as can be seen in Fig. (5.3). Here one can also see that the electron Lorentz factor γ is generally underestimated in the classical case compared to the QED case: the electrons penetrate further into the laser pulse before loosing energy and the energy of the electrons after the collision is greater. The resultant angular spectrum of the radiation can be seen in Fig. (5.4), where one can see that the energy for smaller θ is overestimated by the classical case (here θ represent the angle compared to the propagation direction of the laser pulse).

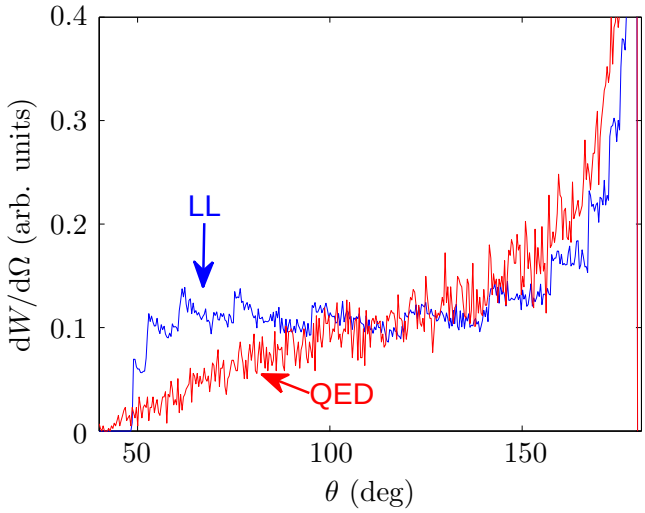

Figure 5.4: The figure shows a comparison between the angular spectra for the QED and LL case.

To understand this effect one must consider the typical direction of radiation emission. It is such that for $a_0 \ll \gamma$ the radiation will be emitted in the forward direction of the electron propagation, for $a_0 \gg \gamma$ it will be emitted in the opposite direction and for $a_0 = 2\gamma$ the predominant direction of emission is perpendicular to the electron propagation direction [44]. Thus, for a given pulse amplitude a_0, the smaller γ is the more the radiation will be concentrated to smaller angles θ (towards the propagation direction of the laser pulse). Thus, as the electron energy is underestimated in the classical case as seen in Fig. (5.3), more energy will be emitted for small θ than in the corresponding QED case.

The described effect was for the idealised case of a Gaussian shaped pulse with a single electron. To see that the observed effect is robust enough to be observed in an experiment we also consider the case of a realistically shaped pulse with a beam of electrons with a spread in energy and position. The result is that indeed, the effect is present also here and thus could work as a signature for en experiment probing radiation reaction.

Chapter 6

Summary of papers

Paper 1

Three-wave interaction and Manley-Rowe relations in quantum hydrodynamics

In this paper we show that the equations for quantum hydrodynamics with a generalized Bohm de Broglie force fulfil the Manley-Rowe relations only for the standard form of the Bohm de Broglie force. This adds further weight to the standard expression for the Bohm de Broglie term, whose derivation to some extent lacks a firm base.

My contribution to this paper was to perform the calculations of the coupled three-wave interaction to show the main result of how the Manley-Rowe relations where fulfilled. I also contributed to deriving the coupled equations for the amplitudes and to writing the paper.

Paper 2

Effects of high energy photon emissions in laser generated ultra-relativistic plasmas: Real-time synchrotron simulations

In this paper we develop a runtime numerical Monte Carlo method for the calculation of the radiation emission spectra for relativistic particles in simulations. We test the method by comparing the emitted energy to the energy loss due to radiation reaction, calculated using the L.L. method, in a particle-in-cell laser wakefield acceleration simulation. The simulations show excellent agreement between the two methods.

My contribution to this paper was to develop and implement the numerical method, run the simulations and to writing the paper

Paper 3

Narrowing of the emission angle in high-intensity Compton scattering

In this paper we implement the same principal ideas for the calculation of the classical radiation spectra of a relativistic particle as used in paper 1, in the one-particle code *Simla* [43]. This simulates the collision of a particle with a realistic laser pulse and is capable of using different equations of motion, including a stochastic QED one. We compare the radiation spectra between runs using a classical equation of motion and runs using a QED equation.

My contribution to this paper was to implement the numerical method for the emission of classical radiation into the single-particle code and contributing to writing a part of the paper.

Acknowledgments

There are many people, family, friends and colleagues I would like to thank for keeping me on track in my work. I would especially like to thanks my supervisors Mattias and Gert for support and for enabling me to continue to work from Umeå. I would also like to thank past and present group members for making work fun, and especially Jens and Arkady for close cooperation. Finally I would like to thank my family and friends, especially Elin and Emil for making life fun.

Bibliography

[1] D. Strickland and G. Mourou. Compression of amplified chirped optical pulses. *Opt. Comm.*, 56(3):219–221, 1985.

[2] V. Yanovsky, V. Chvykov, G. Kalinchenko, P. Rousseau, T. Planchon, T. Matsuoka, A. Maksimchuk, J. Nees, G. Cheriaux, G. Mourou, et al. Ultra-high intensity-300-TW laser at 0.1 hz repetition rate. *Opt. Express*, 16(3):2109–2114, 2008.

[3] J.M. Dawson. Particle simulation of plasmas. *Rev.Mod. Phys.*, 1983.

[4] C.K. Birdsall and A.B. Langdon. Plasma physics via computer simulation. 1985.

[5] J.D. Jackson. Classical electrodynamics. *Classical Electrodynamics, 3rd Edition, by John David Jackson, pp. 832. ISBN 0-471-30932-X. Wiley-VCH, July 1998.*, 1, 1998.

[6] L.D. Landau and E.M. Lifshitz. The classical theory of fields. *Elsevier, Oxford*, 1975.

[7] L. Tonks and I. Langmuir. Oscillations in ionized gases. *Phys. Rev.*, 33(2):195, 1929.

[8] P. Debye and E. Hyckel. De la théorie des électrolytes. i. abaissement du point de congélation et phénomènes associés. *Phys. Zeitz.*, 24(9):185–206, 1923.

[9] D.R. Nicholson. *Introduction to plasma theory*. Cambridge Univ Press, 1983.

[10] A. A. Vlasov. *J. Phys. U.S.S.R.*, 9(25), 1945.

[11] L.D. Landau. On the vibrations of the electronic plasma. *J. Phys. U.S.S.R.*, 10(25), 1946.

[12] J.M. Manley and H.E. Rowe. Some general properties of nonlinear elements-part i. general energy relations. *Proceedings of the IRE*, 44(7):904–913, 1956.

[13] J. Larsson. A new Hamiltonian formulation for fluids and plasmas. part 3. Multifluid electrodynamics. *J. Plasma Phys.*, 55:279–300, 4 1996.

[14] I.Y. Dodin, A.I. Zhmoginov, and N.J. Fisch. Manley–Rowe relations for an arbitrary discrete system. *Physics Letters A*, 372(39):6094–6096, 2008.

[15] E. Wallin, J. Zamanian, and G. Brodin. Three-wave interaction and Manley–Rowe relations in quantum hydrodynamics. *J. Plasma Phys.*, 80(04):643–652, 2014.

[16] J. Lundin, J. Zamanian, M. Marklund, and G. Brodin. Short wavelength electromagnetic propagation in magnetized quantum plasmas. *Phys. Plasmas*, 14:062112, 2007.

[17] F. Haas. *Quantum Plasmas.* Springer, New York, 2011.

[18] G. Manfredi. How to model quantum plasmas. In C. Sulem T. Passot and P.-L. Sulem, editors, *Topics in Kinetic Theory.* Fields Institute Communications, 2005.

[19] G. Manfredi and F. Haas. Self-consistent fluid model for a quantum electron gas. *Phys. Rev. B*, 64(7):075316, 2001.

[20] K.S. Yee et al. Numerical solution of initial boundary value problems involving maxwell's equations in isotropic media. *IEEE Trans. Antennas Propag*, 14(3):302–307, 1966.

[21] B. Gustafsson, H.O. Kreiss, and J. Oliger. *Time dependent problems and difference methods*, volume 24. John Wiley & Sons, 1995.

[22] J.P. Boris. Relativistic plasma simulation-optimization of a hybrid code. In *Proc. Fourth Conf. Num. Sim. Plasmas, Naval Res. Lab, Wash. DC*, pages 3–67, 1970.

[23] F. Peano, M. Marti, L. O. Silva, and G. Coppa. Statistical kinetic treatment of relativistic binary collisions. *Phys. Rev. E*, 79:025701, Feb 2009.

[24] M. Chen, E. Cormier-Michel, C.G.R. Geddes, D.L. Bruhwiler, L.L. Yu, E. Esarey, C.B. Schroeder, and W.P. Leemans. Numerical modeling of laser tunneling ionization in explicit particle-in-cell codes. *J Comput. Phys.*, 236:220–228, 2013.

[25] ELI: www.extreme-light infrastructure.eu.

[26] XCELS: www.xcels.iapras.ru.

[27] Vulcan: www.clf.stfc.ac.uk.

[28] E. Wallin, A. Gonoskov, and M. Marklund. Effects of high energy photon emissions in laser generated ultra-relativistic plasmas: real-time synchrotron simulations. *Phys. Plasmas*, 22:033117, 2015.

[29] C. N. Harvey, A. Gonoskov, M. Marklund, and E. Wallin. Narrowing of the emission angle in high-intensity compton scattering. *Phys. Rev. A*, 93:022112, Feb 2016.

[30] A. Ilderton and G. Torgrimsson. Radiation reaction in strong field QED. *Phys. Lett. B*, 725:481, 2013.

[31] A. Gonoskov, S. Bastrakov, E. Efimenko, A. Ilderton, M. Marklund, I. Meyerov, A. Muraviev, A. Sergeev, I. Surmin, and E. Wallin. Extended particle-in-cell schemes for physics in ultrastrong laser fields: Review and developments. *Phys. Rev. E*, 92:023305, Aug 2015.

[32] A. Gonoskov. Ultra-intense laser-plasma interaction for applied and fundamental physics. *Ph.D. thesis, Umea University*, 2013.

[33] A. Pukhov and J. Meyer-ter Vehn. Laser wake field acceleration: the highly non-linear broken-wave regime. *Appl. Phys. B*, 74(4-5):355–361, 2002.

[34] T. Tajima and J.M. Dawson. Laser electron accelerator. *Phys. Rev. Lett.*, 43(4):267–270, 1979.

[35] P. Sprangle, E. Esarey, a. Ting, and G. Joyce. Laser wakefield acceleration and relativistic optical guiding. *Appl. Phys. Lett.*, 53(22):2146, 1988.

[36] W. Leemans, P. Catravas, E. Esarey, C. Geddes, C. Toth, R. Trines, C. Schroeder, B. Shadwick, J. van Tilborg, and J. Faure. Electron-Yield Enhancement in a Laser-Wakefield Accelerator Driven by Asymmetric Laser Pulses. *Phys. Rev. Lett.*, 89(17):174802, October 2002.

[37] V. Malka, S. Fritzler, E. Lefebvre, and M.M. Aleonard. Electron acceleration by a wake field forced by an intense ultrashort laser pulse. *Science*, 298(November):1596–1601, 2002.

[38] A. Modena, Z. Najmudin, A. Dangor, E., C. E. Clayton, K. A. Marsh, C. Joshi, V. Malka, C. B. Darrow, C. Danson, D. Neely, and F. N. Walsh. Electron acceleration from the breaking of relativistic plasma waves. *Nature*, 377, 1995.

[39] C.G.R. Geddes, C. Toth, and J. Van Tilborg. High-quality electron beams from a laser wakefield accelerator using plasma-channel guiding. *Nature*, 431(September), 2004.

[40] W.P. Leemans, B. Nagler, A.J. Gonsalves, C. Toth, K. Nakamura, C.G.R. Geddes, E. Esarey, C.B. Schroeder, and S.M. Hooker. GeV electron beams from a centimetre-scale accelerator. *Nature Phys.*, 2(10):696–699, 2006.

[41] S. Corde, K. Ta Phuoc, G. Lambert, R. Fitour, V. Malka, A. Rousse, A. Beck, and E. Lefebvre. Femtosecond x-rays from laser-plasma accelerators. *Rev. Mod. Phys.*, 85(1):1–48, 2013.

[42] A. Rousse, K.T. Phuoc, R. Shah, and A. Pukhov. Production of a kev x-ray beam from synchrotron radiation in relativistic laser-plasma interaction. *Phys. Rev. Lett.*, 93(13):135005, Sep 2004.

[43] D.G. Green and C.N. Harvey. Simla: Simulating particle dynamics in intense laser and other electromagnetic fields via classical and quantum electrodynamics. *Computer Physics Communications*, 192:313–321, 2015.

[44] C. Harvey, T. Heinzl, and A. Ilderton. Signatures of high-intensity compton scattering. *Phys. Rev. A*, 79:063407, Jun 2009.